SLAC-PUB-7909
April 2003

Model independent analysis of beam dynamics in accelerators

Chun-xi Wang, John Irwin, Karl Bane, Yunhai Cai, Franz J. Decker, Michiko Minty, Yiton T. Yan *
Stanford Linear Accelerator Center, Stanford University, Stanford, CA 94309

In this paper, we address fundamental issues in BPM-based observations and present methods to analyze beam dynamics in an accelerator. Our analysis methods do not rely on any particular machine model, and therefore are referred to as Model Independent Analysis (MIA). There are two major parts in MIA. One is noise reduction and degree-of-freedom analysis using a singular value decomposition of a BPM-reading matrix. The other is a physical base decomposition of the BPM-reading matrix based on the time structure of pulse-by-pulse beam and/or machine parameters. The combination of these two methods allows one to break the resolution limit set by individual BPMs and observe beam dynamics at more accurate levels. A physical base decomposition is particularly useful for understanding various beam dynamics issues. MIA is a statistical analysis of BPM readings which can be collected non-invasively during normal machine operation, and can lead to better understanding and control of beams.

I. INTRODUCTION

Observation and comprehension of beam dynamics in an operating accelerator is crucial for improving machine performance. The basic information of beam dynamics comes from beam position monitors (BPMs) that measure the beam centroid position. It is usual practice to fit BPM readings to a machine model and calculate various properties such as beta functions, dispersion functions, etc. in order to understand the dynamics and characterize the machine. More advanced techniques based on beam response matrices are often used to calibrate the parameters of one's machine model [1]. A concrete model is essential and fitting the model to observation is the goal.

There are two fundamental issues in BPM-based model-fitting schemes. One is the accuracy limit set by individual BPM resolution, determined by available technology and budget. The other is the accuracy of the model. MIA takes a novel approach to tackle these issues. It is a standard practice to do pulse-by-pulse averaging in order to get more accurate beam orbits. Such time averages are successful in storage rings since there are stable closed orbits and the pulse repetition rate is high. However, in linacs and rings interesting beam dynamics observations often require pulse-by-pulse measurement of beam orbits. A contribution of this paper is to show that one can also improve the resolution limit by taking into account the correlations among a large number of BPM readings. The improvement in observation accuracy may then allow studies of subtle beam dynamics issues and provide better control of the beam.

Since model-fitting approaches rely on the correctness of one's model, they are more suitable when the beam dynamics is well understood, the machine is stable, and a good machine model exists. Often this is not the case. In this paper, we will show how to analyze the beam dynamics without reference to a particular machine model. Basically we apply matrix and statistical analysis methods to systematically analyze the BPM readings for a large number of pulses and a large number of BPMs.

This paper is organized as follows: Section 2 analyzes the BPM readings from a perturbative point of view and discusses the physical base decomposition of a BPM data matrix; section 3 applies the formulation of section 2 to basic orbit fitting problems; section 4 discusses how to improve the BPM resolution limit using a large number of BPMs; Section 5 discusses a singular value decomposition (SVD) [2] or principal components analysis [3] of BPM data; section 6 presents the degree-of-freedom analysis of a beam line; section 7 discusses how to achieve a physical base decomposition using the time structure of pulse signals; section 8 discusses the characteristics of the noise floor of a singular value spectrum; and finally, section 9 describes a kick analysis that is helpful to interpret the physical basis. Most of the plots shown in this paper are the results of experimental data from the linac of the Stanford Linear Collider (SLC). However, MIA can be applied to storage rings as well as linacs. References 2–6 provide a good coverage of the mathematical background for this work.

II. PHYSICAL BASE DECOMPOSITION OF A BPM-READING MATRIX

The central object of MIA analysis is a BPM-reading matrix B, which simply is the data matrix formed by the readings of P pulses on M BPMs (a matrix of P rows and M columns). Physically B contains the transverse beam centroid positions of P pulses sampled by M monitors along a beam line. Clearly, B contains all the information available from BPMs. Let us first examine the physical composition of the matrix B from a perturbative point of view. This is natural since for a short period of time all the pulses are close to an average orbit.

*Work supported by Department of Energy contract DE-AC03-76SF00515.

The transverse beam position of a pulse depends on various physical variables such as the initial incoming conditions of the beam, the settings of magnets, and rf conditions. We can Taylor expand the beam position b over all variables as

$$b = b(\bar{x}_1, \bar{x}'_1, \bar{\delta}, \bar{\sigma}_z, \cdots) + \sum_{v \in \{x_1, x'_1, \cdots\}} \left.\frac{\partial b}{\partial v}\right|_{v=\bar{v}} \Delta v \qquad (1)$$
$$+ \frac{1}{2} \sum_{v_1, v_2 \in \{x_1, x'_1, \cdots\}} \left.\frac{\partial^2 b}{\partial v_2 \partial v_1}\right|_{\substack{v_1=\bar{v}_1 \\ v_2=\bar{v}_2}} \Delta v_1 \Delta v_2 + \cdots$$

where x_1, x'_1, δ, σ_z are respectively the initial beam position, angle, relative energy, and bunch length, given as examples of possible physical variables; the over-bar indicates the expansion points; and $\Delta v = v - \bar{v}$. The zero order term may have a complicated dependency on the variables and is sensitive to unknown BPM offset errors. To eliminate this term, we subtract the average over a large ensemble of pulses and study the difference

$$b - \langle b \rangle = \sum_v \left.\frac{\partial b}{\partial v}\right|_{v=\bar{v}} (\Delta v - \langle \Delta v \rangle) \qquad (2)$$
$$+ \frac{1}{2} \sum_{v_1, v_2} \left.\frac{\partial^2 b}{\partial v_2 \partial v_1}\right|_{\substack{v_1=\bar{v}_1 \\ v_2=\bar{v}_2}} (\Delta v_1 \Delta v_2 - \langle \Delta v_1 \Delta v_2 \rangle) + \cdots$$

where $\langle\ \rangle$ indicates the average over the ensemble of pulses. Although we have found that some second derivatives (which characterize, e.g. the chromatic dependency of the betatron motion) are significant at times, the third and higher order terms are generally negligible and will be dropped (one can easily include more terms when in doubt).[1]

We treat the first and second order terms on the same footing and rewrite Eq.(2) in a concise form

$$b - \langle b \rangle = \sum_{\{q\}} q\, f_q \qquad (3)$$

where the variable $q = \frac{\Delta v - \langle \Delta v \rangle}{\mathrm{std}(\Delta \mathrm{v})}$ or $\frac{\Delta v_1 \Delta v_2 - \langle \Delta v_1 \Delta v_2 \rangle}{\mathrm{std}(\Delta \mathrm{v_1} \Delta \mathrm{v_2})}$ and f_q is the corresponding derivative $\left.\frac{\partial b}{\partial v}\right|_{\bar{v}} \cdot \mathrm{std}(\Delta \mathrm{v})$ or $\frac{1}{2} \left.\frac{\partial^2 b}{\partial v_2 \partial v_1}\right|_{\bar{v}_1, \bar{v}_2} \cdot \mathrm{std}(\Delta \mathrm{v_1} \Delta \mathrm{v_2})$. The physical variables are normalized by their standard deviations over the ensemble of pulses, so that all the q's are dimensionless and reflect the relative changes (otherwise one has to deal with different quantities such as 10^{-5} rad, 10^6 volts, etc.), while all the f's have the same dimension as the BPM readings.

Eq.(3) tells us that a beam orbit is a linear combination of a limited number of "basic" orbits given by the f_q's. In other words, the BPM reading pattern generated by each pulse is a superposition of certain basic patterns. This fact allows us to apply linear algebra concepts and matrix analysis techniques. According to Eq.(3), the BPM-reading matrix B (from now on it consists of $b - \langle b \rangle$ instead of b) which is the ensemble of P pulses monitored with M BPMs can be written as

$$B = Q F^T + N \qquad (4)$$

where matrices $Q_{P \times d} = [\vec{q}_1, \cdots, \vec{q}_d]$, $F_{M \times d} = [\vec{f}_1, \cdots, \vec{f}_d]$, and $N_{P \times M}$ contains the noise associated with each BPM reading. The column vector $\vec{q}_i$ contains the P values of the i-th physical variable and $\vec{f}_i$ contains the M components of the corresponding physical pattern. The q's are referred to as temporal patterns or time structures of pulses, and the f's as spatial patterns or physical vectors. We assume all the physical vectors are linearly independent, i.e. F has full column rank given by d. Neglecting BPM errors, they form a complete basis for the row space of the BPM-reading matrix (i.e. range of B^T). Unlike P and M that can be chosen at will, dimension d is determined by the dynamics. An MIA achievement (see Section 6) is the determination of d. Generally d is a small number and we choose P and M so that $d \ll M \ll P$ to obtain statistical benefits. Typical numbers are $d \sim 10$, $M \sim 10^2$, and $P \sim 10^3$.

The matrix F contains (stationary) beam-line properties such as the dispersion function. Matrices Q and N contain stochastic quantities that change from one ensemble to another. However, $\frac{1}{P} Q^T Q = C_Q$, which is the standard correlation matrix of the q variables, contains statistical properties of the ensemble of pulses. Thus, if everything is stable, C_Q contains only stationary machine properties. Similarly, $\frac{1}{P} N^T N$ characterizes BPM resolutions as well as possible correlations in BPM noise. For convenience, we normalize B, Q, and N by $\sqrt{P}$, so that the important (variance-)covariance matrix of BPM readings and the correlation matrix of temporal signals (q's) can be formed simply as

$$C_B = B^T B \quad \text{and} \quad C_Q = Q^T Q. \qquad (5)$$

Note that the statistical meaning of Eq.(5) requires that the column means of B and Q have been taken out. Obviously

$$C_B = F\, C_Q F^T \qquad (6)$$

if one neglects noise. This shows the mathematical relationship between C_B and C_Q.

We call Eq.(4) a physical base decomposition of the BPM-reading matrix. Although straightforward, it is an

[1] Concentrating for a moment on just the initial conditions as variables, a standard map formalism yields

$$\vec{z}(s) = \sum_{\vec{n}} \vec{R}_{\vec{n}}(s_0 \to s) \cdot z_0^{\vec{n}}.$$

Each $\vec{R}_{\vec{n}}(s_0 \to s)$ is a possible physical vector. Since in a ring the z_0 changes in each turn, with sufficient resolution and orbit amplitudes, one might hope to observe the $\vec{R}_{\vec{n}}(s_0 \to s)$.

important statement both conceptually and mathematically. It also contains the goal of MIA: to find F from measured B and Q. Physically speaking, the major goals of beam dynamics analysis are:

- identify a complete set of variables contributing to the beam motion and the physics behind them;
- determine all the physical-basis patterns and the physics behind them.

To achieve these objectives, it is essential to isolate signals from noise. In the following sections, we will discuss how to handle N, find d, and obtain F.

Physical base decomposition is not unique in the sense that one can choose physical variables differently. Therefore the BPM-reading matrix itself does not contain sufficient information for us to achieve the decomposition we want. Extra information about the physical variables is necessary. Although it is possible to impose certain mathematical requirements (such as orthogonality) to make the decomposition unique, such a decomposition will have limited use.

III. GENERAL ORBIT FITTING FORMULA

Before focusing on MIA, we apply Eq.(4) to the conventional orbit-fitting problems based on a machine model and present general orbit fitting formula. This will help to illustrate the meaning of Eq.(4) and serve as a review of this basic issue in beam dynamics observations. As a basic tool, orbit fittings are used to measure beam parameters such as position, angle, relative energy, and so on. Such problems can be accommodated easily into Eq.(4) by setting $P = 1$. F is supposedly given by the machine model and the job is to find the corresponding beam parameters in Q. When the number of BPMs is larger than the degrees of freedom ($M > d$), least-squares fitting is used to find the best solution:

$$Q = BF(F^T F)^{-1} \tag{7}$$

and the error is $NF(F^T F)^{-1}$, where we have assumed that BPMs have the same resolution σ_n and their noises are independent (i.e. $N^T N = \sigma_n^2 I$), otherwise a more complex formula is necessary for a least-squares solution [6]. Note that Eq.(7) covers the $M = d$ case as well. The variance-covariance matrix of errors in Q can be computed as

$$\left\langle \left[NF(F^T F)^{-1}\right]^T NF(F^T F)^{-1} \right\rangle_{\text{noise}} = \sigma_n^2 (F^T F)^{-1}. \tag{8}$$

Square roots of the diagonal terms give rms errors of the measurement due to noise, which can be easily calculated from the given F. Two general conclusions can be drawn from Eq.(8) without knowing the details of F: 1) $F^T F$ had better be well conditioned; 2) Since $F^T F$ generally increases with M (i.e. $F^T F/M$ tends to be a constant, at least for a periodic lattice as in a beam line), the measurement error goes down as $\frac{1}{\sqrt{M}}$. Therefore one can reduce the BPM random noise effects on the measurement by using more and more BPMs. However, in addition to the random noise, the accuracy of the machine model specified in F is crucial for an accurate measurement.

Now let us consider a familiar example. For an ideal 2D linear lattice, the beam position at the n-th BPM x_n is given by the R-matrices as $x_n = R_{11}(n)x_0 + R_{12}(n)x_0'$. Suppose we measure a pulse at M BPMs and know the transformation matrix R's from some model, and wish to fit the orbit to the model and find the initial x_0, x_0' of the orbit. In this case, $B = QF^T$ becomes

$$[x_1, x_2, \cdots, x_M] = [x_0, x_0'] \begin{bmatrix} R_{11}(1) & R_{12}(1) \\ R_{11}(2) & R_{12}(2) \\ \vdots & \vdots \\ R_{11}(M) & R_{12}(M) \end{bmatrix}^T \tag{9}$$

and the transpose of Eq.(7) yields

$$\begin{bmatrix} x_0 \\ x_0' \end{bmatrix} = \begin{bmatrix} \vec{R}_{11}\cdot\vec{R}_{11} & \vec{R}_{11}\cdot\vec{R}_{12} \\ \vec{R}_{12}\cdot\vec{R}_{11} & \vec{R}_{12}\cdot\vec{R}_{12} \end{bmatrix}^{-1} \begin{bmatrix} \vec{R}_{11}\cdot\vec{x} \\ \vec{R}_{12}\cdot\vec{x} \end{bmatrix} \tag{10}$$

where $\vec{x}$ consists of the orbit, $\vec{R}_{11}$ consists of the R_{11}'s, and so on. The 2×2 matrix inversion can be done analytically and leads to the expressions seen in the literature [7]. It is obvious how to include more degrees of freedom via Eq.(7) or by extending Eq.(10) directly.

IV. BREAKING THE PULSE-BY-PULSE RESOLUTION LIMIT

In beam dynamics experiments, one often encounters BPM resolution problems. Sometimes simple pulse-by-pulse averaging can improve accuracy. But often single-pulse measurements with resolution better than the BPM resolution are desirable. In this case, the only option left is some sort of average over a large number of BPMs. Were there M identical BPMs at the same location to monitor the beam position, averaging these BPM readings would improve the measurement by a factor of $\frac{1}{\sqrt{M}}$. In reality, one has many BPMs distributed along a beam line. The question is: even though we do not know the exact relations among BPM readings for a pulse, can we take advantage of the potential statistical benefits of using a large number of BPMs?

This can be achieved from a SVD analysis of the BPM-reading matrix. The method is fairly simple: compute the singular value decomposition of $B = USV^T$, set the singular values due to noise to zero to form the noise-cut $\underline{S}$, then recompute $U\underline{S}V^T$. The resulting matrix has a noise term reduced by $\sqrt{d/M}$ where d is the dimension of signal space. In the following sections, we will discuss the SVD in detail and show how to identify the singular values due to noise.

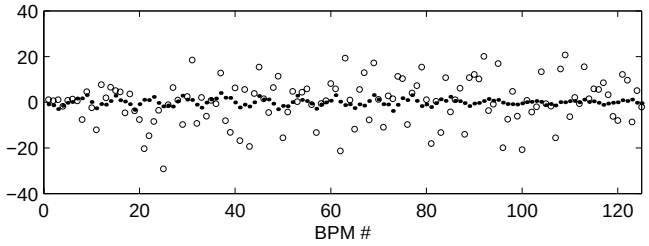

FIG. 1. Effect of cutting noise

Figure 1 demonstrates the effect of the noise-cut. 5000 pulses over 125 BPMs were generated to simulate various signals in SLC. Then random noise, 1 μm for the first 7 and 10 μm for the rest BPMs, was added. After cutting the noise, the residual noise was obtained by subtracting the signals from the noise-reduced matrix. Figure 1 plots the added noise in circles and residual noise in dots for the first pulse. Results for all other pulses are similar. It is remarkable that this simple procedure can significantly reduce the random noise of each individual BPM reading. In other words, we can improve BPM resolution individually by using a large number of BPMs and sufficiently large number of pulses. Though simple and powerful, this method seems not to have been used before for beam dynamics analysis. However, a similar method (i.e. setting signal instead of noise singular values to zero) has been used for estimating BPM resolutions [8].

V. SINGULAR VALUE DECOMPOSITION

In this section we focus on the physical and statistical meaning of the SVD results in order to illustrate their usefulness and limitations for beam dynamics analysis.

Mathematically, an SVD of the matrix B yields

$$B = USV^T = \sum_{i=1}^{d} \sigma_i u_i v_i^T \qquad (11)$$

where $U_{P\times P} = [u_1, \cdots, u_P]$ and $V_{M\times M} = [v_1, \cdots, v_M]$ are orthogonal matrices, $S_{P\times M}$ is a diagonal matrix with nonnegative σ_i along the diagonal in nonincreasing order. $d = \mathrm{rank}(B)$ is the number of nonzero singular values. σ_i is the i-th largest singular value of B and the vector u_i (v_i) is the i-th left (right) singular vector. Often (assuming $M < P$ since we are interested in overdetermined system only) a trimmed down version is used, in which only the first M columns of U and the first M rows of S are kept. The singular values are uniquely determined and the singular vectors corresponding to the distinct singular values are determined up to a sign. The singular values reveal information of the matrix rank while each set of singular vectors form an orthogonal basis of the various spaces of the matrix. These properties make the SVD extremely useful. There are direct relationships between SVD and the eigenvalue problem of real symmetric matrices, which can be seen from

$$B^TB = VS^2V^T \quad \text{and} \quad BB^T = US^2U^T, \qquad (12)$$

i.e. the column vectors of V (U) are eigenvectors of the real symmetric matrix B^TB (BB^T) with eigenvalues given by the corresponding diagonal term σ_i^2's.

Since B^TB is the covariance matrix of BPM readings, SVD in fact accomplishes the principal components analysis of BPM readings. Unlike the physical base decomposition given in Eq.(6), the orthogonal base decomposition in Eq.(12) is uniquely determined by B. From this we can conclude that both the singular values (in S) and the right singular vectors (in V) should be repeatable for different ensembles of pulses, providing that the machine is stable (i.e. all machine conditions are the same). On the other hand, the U matrix will change from one ensemble to another because BB^T does not represent a stationary statistical property of the system.

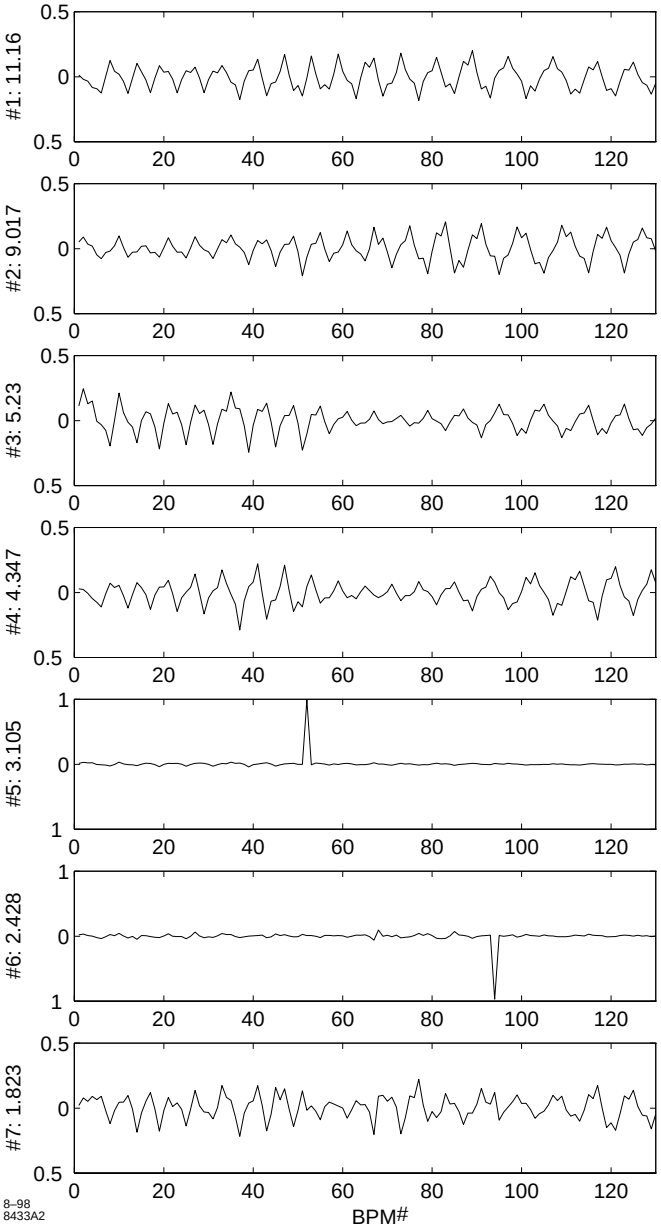

FIG. 2. Singular-vector plot

Figure 2 shows the first 7 singular vectors and corresponding singular values (in μm on the left labels). The experimental data are horizontal BPM readings from SLC linac for 5000 pulses and 130 BPMs. We see that the singular values go down quickly from about 10μm to 1μm. Therefore at a 1μm coherent signal level, all the motions observed in B would be a linear combination of less than 10 modes. We will examine the remaining singular values in the next section. The most striking patterns are modes #5 and #6. Clearly they are due to individual BPMs. This example shows that one can easily identify problematic BPMs, valuable information for any beam control and dynamics study. The top 2 modes are significantly larger than the rest. They are mainly due to the 2 degrees of freedom in the horizontal betatron motion.

Although such singular-vector plots yield valuable information such as the location of noisy BPMs, it has limited use otherwise, since the orthogonal decomposition often mixes various different physical effects. As mentioned earlier, extra information is required to determine the physical base decomposition. Nonetheless, the orthogonal base decomposition provides an important step towards physical base decomposition.

To understand the meaning of singular values in MIA, we write $B^T B$ as

$$\sum_{i=1}^{d} \sigma_i^2 v_i v_i^T = \begin{bmatrix} \mathrm{var(BPM_1)} & \mathrm{cov(BPM_{12})} & \cdots \\ \mathrm{cov(BPM_{21})} & \mathrm{var(BPM_2)} & \cdots \\ \vdots & \vdots & \ddots \end{bmatrix} \quad (13)$$

Comparing diagonal terms we have

$$\mathrm{var(BPM}_k) = \sum_{i=1}^{d} \sigma_i^2 \; v_i(k)^2, \qquad k = 1, \cdots, M \quad (14)$$

and

$$\sum_{k=1}^{M} \mathrm{var(BPM}_k) = \sum_{i=1}^{d} \sigma_i^2. \quad (15)$$

These equations confirm that the variance of the k-th BPM readings is the sum over the i modes with $\sigma_i^2 \; v_i(k)^2$ from each. Of course the square of a singular value is the sum of the variances of BPM readings due to the corresponding mode. Since a spatial vector v_i is normalized to unity, for a coherent signal $v_i^2(k) \sim \frac{1}{M}$, hence $\sigma_i^2 \sim M$. For a localized BPM noise, $v_i^2(k)$ is constant and so is σ_i^2. We often use normalized singular values $\hat{\sigma}_i \equiv \frac{\sigma_i}{\sqrt{M}}$ since they reflect the average amplitudes of signals. Under this normalization, $\hat{\sigma}_{\mathrm{signal}}$ is roughly constant with changing M while $\hat{\sigma}_{\mathrm{noise}} \propto \frac{1}{\sqrt{M}}$.

VI. DEGREE OF FREEDOM ANALYSIS

In any dynamical system, the degrees of freedom of the system offers very basic information about the dynamics. Roughly speaking, it reflects how many things are independently changing. A simple example can illustrate why it is important to analyze the degrees of freedom in a beam line. Suppose one has an "ideal" beam line (like the example used in section 3) and that there is no coupling between horizontal and vertical planes, no significant nonlinearities, etc., then the only possible motions are betatron motions excited by the initial beam position and angle. It is clear that there are only 2 degrees of freedom (usually characterized by the so called sine-like and cosine-like trajectories) available in the system. Now, suppose one of the corrector magnets in the beam line malfunctions and drifts around, it will kick the beam and excite an independent betatron motion starting at the corrector. Analyzing such a system, one will find 3 independent BPM patterns instead of 2. Furthermore, one can try to find where the new degree of freedom starts, and therefore locate the jitter source. We will formalize such an idea below.

Firstly we discuss how to determine d, the degrees of freedom, after measuring the BPM-reading matrix B for a sufficiently large ensemble of pulses. Mathematically, this is the same as finding rank(B). Such a fundamental question has a well-known answer: check the singular values of B in the SVD of the matrix. If there is no noise, the number of nonzero singular values gives the d value. In practice, one has to find the noise level and set up a criteria to determine which singular values are significant. This is a subtle issue which we will address in a separate section. Here we simply show one typical singular-value plot from SLC linac data. Note that in singular-value plots, we use normalized singular values ($\hat{\sigma}$'s), so that the singular values of the signals reflect their average rms strengths. Figure 3 plots all singular values of the data set used in Figure 2. It shows that most of the singular values are small and about the same size. They are due to BPM noise. Thus the long flat part is called the noise floor. It has interesting characteristics which we will describe later. Above the noise floor, there

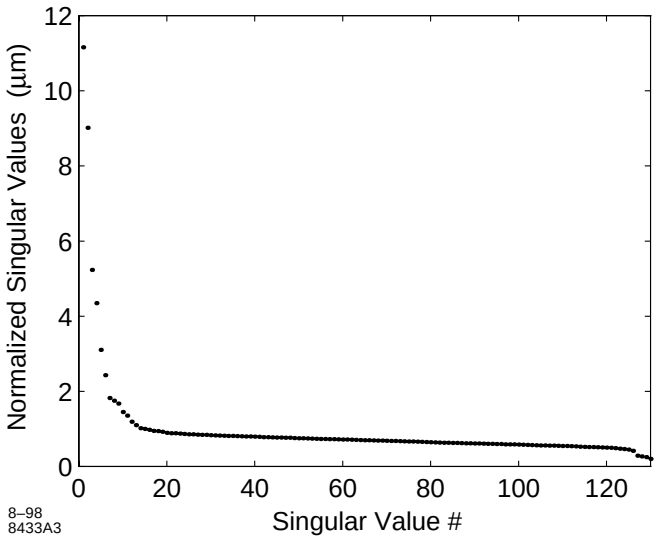

FIG. 3. Singular-value plot

are about 10 singular values. As shown in Figure 2, some of those are due to large individual BPM noise instead of beam dynamics. Even so, there are still more degrees of freedom in this system than assumed by the typical online machine models. In other words, a traditional model-fitting approach is bound to miss important dynamics in this beam line.

It is useful to trace the increase of the number of degrees of freedom along the beam line using SVD analyses of an increasing number of BPM readings. Such a systematic SVD analysis can reveal the locations where new degrees of freedom appear. These locations could be a jittering source such as a varying corrector, or a structure misalignment that shows up as a jittering source because of current jitter, and so on. Figure 4 is an example of such a plot (using the same data set of Figure 3 including only the top 10 singular values), which we call a "degree-of-freedom plot". Unlike Figure 3, the singular values plotted here are not normalized by the number of BPMs. (thus one must divide the ending values in Figure 4 by $\sqrt{130}$ in order to get the first 10 points of Figure 3). There are many general features in a degree-of-freedom plot of a normal running beam line. Modes due to random noise yield flat lines, while coherent signals grow with the number of BPMs used. The slope of a curve indicates the local strength of that signal. Usually, there are two curves on the very top of the plot well separated from the rest. They are mainly due to the 2 betatron modes. Sometimes, there is only one curve because the other mode is hardly excited due to beam injection constraints. There are small wiggles on most of the curves, which are the result of periodic lattice function changes. The key value of a degree-of-freedom plot is to analyze the appearance of new degrees of freedom, and the exact values are not that important since they most often do not correspond to strengths of physical modes (see discussion on orthogonal basis in the previous section).

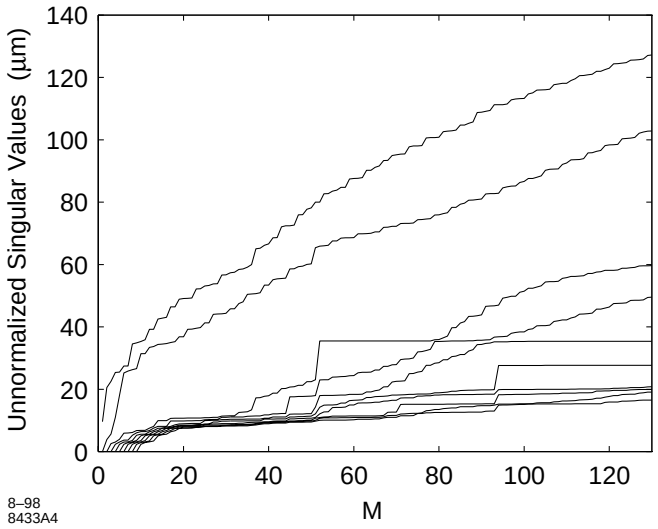

FIG. 4. Degree-of-freedom plot

If a mode is due to an individual BPM, we will see a curve like a step function starting at that BPM. The step level indicates the noise magnitude. There are 3 such cases clearly shown in Figure 4 (all noisy BPMs are kept in order to show their effects). There is a baseline in a degree-of-freedom plot, which reflects the BPM resolution. In this example, the BPM resolutions are about 10 μm. The beginning slope of eigenvalues 3–10 is special to this example, since we have several high resolution BPMs at the beginning of the linac. (however, at least $M \geq d$ is needed to establish various modes, thus the points within the first few BPMs are only useful to determine initial betatron amplitudes.)

Before leaving this section, we mention that instead of using more and more BPMs as shown above, one can analyze various subsets (e.g. every 10 BPMs) of all BPMs and locate where new degrees of freedom appear. However, this approach loses the advantage of using large number of BPMs, and may have more trouble detecting weak signals. Though this problem may be alleviated by cutting noise as described before, there are physical patterns which look very much like a betatron motion locally and will be degenerate in a localized degree-of-freedom analysis.

VII. PHYSICAL BASE DECOMPOSITION VIA TIME STRUCTURE OF PULSE SIGNALS

As we mentioned earlier, the orthogonal bases obtained from SVD are often a mixture of various physical patterns and therefore hard to interpret. Extra information is necessary to achieve a physical base decomposition. In a beam line, in addition to the transverse beam positions, there are various kinds of pulse-by-pulse beam and machine parameters that can be monitored. At SLC, for example, we can monitor beam current, bunch length, incoming beam (longitudinal) phase, relative beam energy, klystron phases along the linac, and so on. This section will discuss how to take advantage of such information.

Mathematically, this problem is similar to the orbit fitting problem discussed earlier. Instead of knowing F, we know Q (or a subset of it) and wish to solve for F. If we knew all the physical variables with sufficient accuracy, the corresponding physical basis could be computed as

$$F^T = C_Q^{-1} Q^T B + O(\frac{1}{\sqrt{P}}). \tag{16}$$

This expression emphasizes the importance of underlying correlations among the observed variables.

Note that the accuracy of Eq.(16) does not rely on the number of BPMs used. It simply fits the readings of each BPM to various temporal patterns individually and ignores any correlations among BPM readings. As we discussed earlier, the BPM noise can be reduced statistically by taking into account the correlations among BPM

readings. Therefore, if we cut the noise first and then apply Eq.(16), the noise level can potentially be reduced by a factor of $\frac{1}{\sqrt{M}}$, and we have

$$F^T = C_Q^{-1} Q^T U \underline{S} V^T + O(\sqrt{\frac{d}{P\,M}}) \tag{17}$$

where USV^T is the SVD of B, and $\underline{S}$ indicates the zeroing of small singular values that are due to noise. However, this statistical error limit (60 nm in our case) may be hard to achieve due to problems such as machine instability and incomplete information in Q. Nonetheless it indicates the inherent potential sensitivity of this method.

Usually we know only a subset of Q, say Q_s of $Q = [Q_s, Q_r]$. We can still calculate F_s according to Eq.(16) with Q_s, The error due to the missing part is

$$(F_s - F_s^{\rm exact})^T = (Q_s^T Q_s)^{-1} Q_s^T Q_r F_r^T \tag{18}$$

Therefore, if the known subset Q_s is uncorrelated with the remaining unknown temporal patterns, i.e. $Q_s^T Q_r = 0$, then we would obtain the same results as if we had measured all Q. Otherwise, the unknown part of the physical basis (i.e. F_r) will be mixed into the measured parts. This can be a limitation of a totally non-invasive procedure. However, many known physical variables can be slightly modulated on purpose (incoming position, bunch length, and longitudinal phase, for example). In this way the patterns due to these changeable variables can be identified and the patterns corresponding to unknown or unchangeable variables can be further clarified. Then, one will change additional suspected variables in search for these unknowns.

Often the measured temporal patterns of certain physical variables have limited accuracy due to measurement difficulties. To evaluate the effect of such errors, let us assume the measured signals are $Q + \Delta Q$ where ΔQ represents the error, then the error in F can be written as

$$\begin{aligned} \Delta F^T &\equiv C_{Q+\Delta Q}^{-1} (Q + \Delta Q)^T B - F^T \\ &= -C_{Q+\Delta Q}^{-1} \Delta Q^T \Delta Q \; F^T \end{aligned} \tag{19}$$

where we have assumed that the measurement errors ΔQ are independent of Q, i.e. $Q^T \Delta Q = 0$. Eq.(19) shows that the errors in temporal pattern measurement come into play mainly at the second order. Therefore, it is more tolerable than BPM errors. Furthermore, if we know the variance-covariance $\Delta Q^T \Delta Q$ of the measurement errors,[2] Eq.(16) can be modified to take Q errors into account via

$$F^T = \left(I - C_{Q+\Delta Q}^{-1} \Delta Q^T \Delta Q \right)^{-1} C_{Q+\Delta Q}^{-1} (Q + \Delta Q)^T B \tag{20}$$

[2] Of course we have no way to know ΔQ, but statistical characteristics such as $\Delta Q^T \Delta Q$ may be obtained through equipment calibrations.

Note that all the quantities in this expression are measurable.

Eq.(16) is mathematically the same as Eq.(7) but they are different physically, and it turns out to be very useful in the measurement of physical-basis patterns. Eqs. (16) and (18) seem to have never been used before, at least not in this generalized form.

VIII. NOISE FLOOR CHARACTERISTICS

We claimed earlier that the singular values in the flat floor (as shown in Figure 3) of a singular-value plot are due to BPM noise. In this section we will confirm that those singular values indeed behave like noise. First of all, without the noise term in Eq.(4), the rank of B will be d. Since physically we do not expect a large d, most of the singular values should be zero if not due to noise. More convincing evidence comes from the statistical characteristics of the noise floor. We can examine the data and see how the noise floor behaves when changing BPM number M and pulse number P.

Figure 5 shows the dependency on M. In the top frame the 4 curves represent the singular values of the same 5000 pulses but with 30, 60, 90, 120 BPMs respectively. In addition to the general appearance of a noise floor (i.e. a long flat part and small tails at ends), the noise levels indeed decrease with increasing M. The bottom frame plots in circles the inverse square of the median values of the above 4 curves vs. M. The solid line is a linear fit. Such $\frac{1}{\sqrt{M}}$ dependency indicates that the long tail in the singular-value plot is indeed due to random noise, since coherent signals will have roughly the same singular values as M increases. Note that, were there other distributed sources of random noise (such as dark

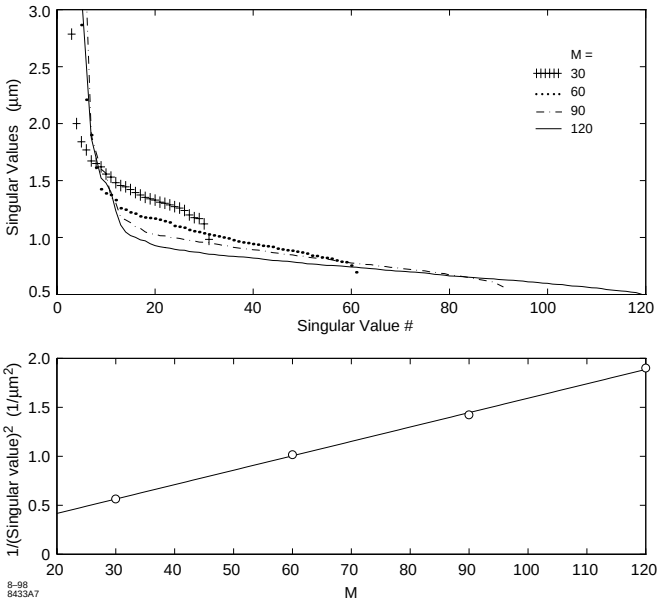

FIG. 5. M dependency of noise floor

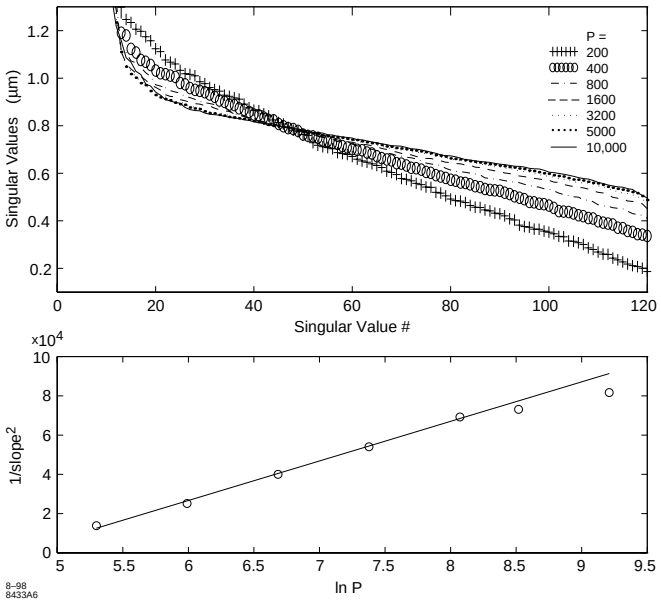

FIG. 6. P dependency of noise floor

current in accelerator structures) affecting the measurement, the noise floor would not decrease as $\frac{1}{\sqrt{M}}$.

Figure 6 shows the noise floor dependency on P. The first frame plots respectively singular values of 7 ensembles of 200, 400, 800, 1600, 3200, 5000, 10000 pulses, with $M = 120$ for all cases. It shows that the slope of the noise floor decreases with increasing P, while the noise levels stay the same at a roughly fixed point. The second frame plots the variance of the eigenvalues (except the first 15) vs. P. The circles correspond to the above 7 noise floors and the solid curve is a least-squares fit to a second order polynomial in $\frac{1}{\sqrt{P}}$, which is the expected P dependency as explained in the appendix. We see that the measured data fit our statistical noise model very well except the first point ($P = 10000$). This discrepancy indicates that the statistical noise due to sample size P is negligible at this level. At about 5000 pulses the slope reaches a limit, which we suspect to be the intrinsic resolution spread among the BPMs. Thus the noise floor of the singular-value plot reflects the BPM resolution spectrum, provided that the pulse ensemble is sufficiently large.

From the fixed point in the top frame, the average BPM resolution is about $\sqrt{120} * 0.8 = 9\mu m$. From the slope, the resolution spread is estimated at about 2 μm. To estimate the resolution of individual BPMs, one can use the method mentioned at the end of section 4. The little tail at the very end of Figure 3 arises from several high resolution BPMs at the beginning of the beam line. We deliberately removed those BPMs from the data in Figures 5 and 6 for clarity.

Simulation studies of noise-only cases show the same M and P dependencies. Therefore the singular-value floor must be due to the BPM noise, though it is still possible that there are small coherent signals buried in this noise floor.

IX. KICK ANALYSIS OF PHYSICAL BASIS

After the physical bases are obtained, most of the base vectors look like betatron oscillations because no matter what the physical sources, the resultant motion of the beam centroid is usually a sum of excited betatron oscillations. We can analyze them further for better understanding with a kick analysis. The goal is to identify the source kicks that generate the physical patterns. The basic idea has two ingredients: kick representation and removal of betatron response due to the lattice. The kick representation is just an equivalent representation of the same vector. Instead of giving the resultant motion, the kick representation simply shows the kicks which cause the motion. Since forces (which cause momentum changes) are much more likely to be localized along a beam line, the kick representation of a physical base usually has a simpler structure and reveals the location of the sources contributing to the motion.

There are many ways to accomplish kick analysis. We describe a simple method here. Assume the betatron basis are given by f_1 and f_2, and a physical pattern g is to be analyzed. For any 3 consecutive points (which form vectors $\vec{f_1}$, $\vec{f_2}$ and $\vec{g}$), use the first 2 points to find a combination of the betatron basis that fits the first 2 points of g (which is always possible) and then predict what the 3rd point of g should be if it follows a betatron oscillation. The differences, which could be computed[3] via

$$\Delta z = \frac{(\vec{f_1} \times \vec{f_2}) \cdot \vec{g}}{(\vec{f_1} \times \vec{f_2})_3}, \tag{21}$$

are assigned to the corresponding BPMs as the result of a kick analysis of g. Δz gives the exact beam displacement due to potential kicks.

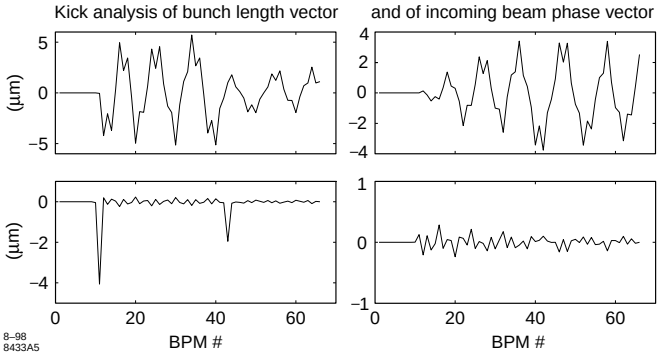

FIG. 7. Examples of kick analysis of physical basis

[3] the described concept can be represented by the simple formula $\vec{g} = \alpha\vec{f_1} + \beta\vec{f_2} + \Delta z\,(0, 0, 1)$ where α, β, and Δz are coefficients. A dot product of $\vec{f_1} \times \vec{f_2}$ to both sides yields Δz.

Figure 7 shows two examples of a kick analysis in a simulation study, in which there are two 300 μm structure misalignments, 10% bunch length jitter, and 0.5° incoming beam (longitudinal) phase jitter (in addition to the betatron oscillations etc.). The top two plots are the two vectors corresponding to the bunch length and incoming beam phase jittering respectively. The bottom two plots give the kick analysis of the two base vectors according to Eq.(21). Although the two base vectors look rather similar (like other betatron oscillations as well), the kick analysis yields completely different characteristics. The bunch length vector is clearly the result of two major localized wakefield kicks generated by the two structure misalignments. The kick analysis shows nicely the locations and strengths. The strength difference is due to the energy dependency of the wakefield kick. On the other hand, the incoming beam phase vector does not consist of any major kicks at all, because the wakefield kicks are not sensitive to the incoming beam phase change (the effect of beam energy change is rather weak). The apparent oscillation is due to the energy dependency of the betatron oscillation frequency. The wakefield kicks merely launches the oscillation, which then grows with the increase of the accumulated betatron phase difference.

X. CONCLUSION

We have presented methods (under the title Model-Independent Analysis–MIA) to analyze beam dynamics without resorting to any particular machine model. The main feature of MIA is a systematic statistical analysis of a BPM-reading matrix (B). By taking advantage of correlations among a large number of BPM readings, one can easily identify problematic BPMs and significantly reduce the effects of BPM random noise. The degree-of-freedom analysis of a beam line provides valuable information on potential jitter sources that may be due to unknown physics or malfunctioning machine components. The physical base decomposition of a noise-reduced matrix via measurable physical variables can be used to extract various physical patterns with greatly enhanced sensitivity and impossible to obtain otherwise. Further analysis (such as kick analysis) of the physical patterns can facilitate the interpretation of the results. Therefore we believe MIA can advance beam observation and dynamics analysis and lead to better control of a beam.

ACKNOWLEDGEMENT

We would like to thank M. Ross and N. Phinney as well as the SLC operation crew for their support. Special thanks is due to L. Hendrickson for her updating the SLC solo control program (SCP) to support our data acquisition. We would also like to acknowledge A. Chao, M. Lee, P. Raimondi, S. Smith, and P. Tenenbaum for helpful discussions.

[1] See for example, W. J. Corbett, M. J. Lee, V. Ziemann, Proceedings of Particle Accelerator Conference 1993, p.108; J. Safranek, Nucl. Instr. and Meth. A 388 (1997)27-36.

[2] Gene H. Golub and Charles F. Van Loan, Matrix Computations, 3rd edition, The Johns Hopkins University Press 1996

[3] R. Gnanadesikan, Methods for Statistical Data Analysis of Multivariate Observations, 2nd edition, John Wiley & Sons, INC. 1997

[4] Charles L. Lawson and Richard J. Hanson, Solving Least Squares Problems, Prentice-Hall, Inc. 1974

[5] T. W. Anderson, An Introduction to Multivariate Statistical Analysis, 2nd edition, John Wiley & Sons, Inc. 1984

[6] Walter C. Hamilton, Statistics in Physical Science, The Ronald Press Company 1964

[7] See for example, R. Assmann, et al. LIAR–A computer program for the modeling and simulation of high performance linacs, SLAC internal report, AP-103

[8] Steve Smith, (unpublished) private communication

APPENDIX

In this appendix, we derive expressions for the mean and variance of the eigenvalue λ's of the variance-covariance matrix C_B in order to understand the P dependency of noise floor. At $P = \infty$ we have the decomposition $\hat{C}_B = \hat{V}\hat{\Lambda}\hat{V}^T$, where $\hat{}$ indicates the $P \to \infty$ quantities and $\hat{\Lambda} \equiv \mathrm{diag}(\hat{\lambda}_1, \cdots, \hat{\lambda}_M)$. For a finite P, statistical noise will result in slightly different C_B, V, and eigenvalues. However $\hat{V}^T C_B \hat{V}$ should still be close to $\hat{\Lambda}$. Let $\hat{V}^T C_B \hat{V} = \hat{\Lambda} + \mathcal{E}$, where the symmetric matrix $\mathcal{E} \equiv \{\epsilon_{ij}\}$ represents the difference due to statistical noise. Taking trace of both sides yields

$$\mathrm{tr}(C_B) = \sum_{i=1}^{M} \lambda_i = \sum_{i=1}^{M} \hat{\lambda}_i + \sum_{i=1}^{M} \epsilon_{ii} \tag{22}$$

Multiplying the transpose of each side to itself and then taking trace yields

$$\mathrm{tr}(C_B^T C_B) = \sum_{i=1}^{M} \lambda_i^2 = \sum_{i=1}^{M} \hat{\lambda}_i^2 + 2\sum_{i=1}^{M} \hat{\lambda}_i \epsilon_{ii} + \sum_{i,j=1}^{M} \epsilon_{ij}^2 \tag{23}$$

Combine these two equations we have

$$\mathrm{var}(\lambda) = \mathrm{var}(\hat{\lambda}) + \frac{1}{M}\sum_{i,j=1}^{M} \epsilon_{ij}^2 + \frac{2}{M}\sum_{i=1}^{M} \Delta\hat{\lambda}_i\, \epsilon_{ii} - \left(\frac{1}{M}\sum_{i=1}^{M} \epsilon_{ii}\right)^2 \tag{24}$$

where $\Delta\hat{\lambda} \equiv \hat{\lambda} - \langle\lambda\rangle$. The last term is obviously much smaller then the second term and can be dropped. Thus the difference in mean value and variance due to statistical noise can be expressed as

$$\langle\lambda\rangle - \langle\hat{\lambda}\rangle = \frac{1}{M}\sum_{i=1}^{M}\epsilon_{ii} \tag{25}$$

$$\mathrm{var}(\lambda) - \mathrm{var}(\hat{\lambda}) \simeq \frac{1}{M}\sum_{i,j=1}^{M}\epsilon_{ij}^2 + \frac{2}{M}\sum_{i=1}^{M}\Delta\hat{\lambda}_i\,\epsilon_{ii}$$

Since both diagonal term ϵ_{ii} and off-diagonal term ϵ_{ij} have $\frac{1}{\sqrt{P}}$ dependency for large P, the differences vanish when $P \to \infty$ as they should. The mean value approaches to the real value in a typical $\frac{1}{\sqrt{P}}$, while the variance behaves more complicated. For small P and $\Delta\hat{\lambda}$, the first term dominates and yields a $\frac{1}{P}$ dependency. As P becomes sufficiently large, the second term will become dominate and results in a $\frac{1}{\sqrt{P}}$ dependency, provided that the system is sufficiently stable. The summations in these expressions can greatly suppress the fluctuation due to statistical quantity ϵ's, thus we can expect a clear P dependency even for small number of pulses.

Note that similar behavior will hold for the singular-values as long as the eigenvalue spread is sufficiently small. Also note that the slope of the noise floor is proportional to the standard deviation of the singular-values as long as the noise floor is flat.